ACS APPLIED MATERIALS & INTERFACES

Research Article

www.acsami.org

Surface Modification of TiO_2 Photoanodes with Fluorinated Self-Assembled Monolayers for Highly Efficient Dye-Sensitized Solar Cells

Sanghyuk Wooh,[†,‡,¶] Tea-Yon Kim,[§,¶] Donghoon Song,[§] Yong-Gun Lee,[†,‡] Tae Kyung Lee,[§] Victor W. Bergmann,[∥,#] Stefan A. L. Weber,[∥,#] Juan Bisquert,[⊥,△] Yong Soo Kang,[*,§] and Kookheon Char[*,†,‡]

[†]The National Creative Research Initiative Center for Intelligent Hybrids and [‡]The WCU Program of Chemical Convergence for Energy and Environment, School of Chemical and Biological Engineering, Seoul National University, Seoul 02268, Korea

[§]Department of Energy Engineering and Center for Next Generation Dye-Sensitized Solar Cells, Hanyang University, Seoul 133-791, Korea

[∥]Max Planck Institute for Polymer Research, 55128 Mainz, Germany

[⊥]Institute of Advanced Materials (INAM), Universitat Jaume I, 12006 Castelló, Spain

[#]Institute for Physics, Johannes Gutenberg University, 55128 Mainz, Germany

Supporting Information

ABSTRACT: Dye aggregation and electron recombination in TiO_2 photoanodes are the two major phenomena lowering the energy conversion efficiency of dye-sensitized solar cells (DSCs). Herein, we introduce a novel surface modification strategy of TiO_2 photoanodes by the fluorinated self-assembled monolayer (F-SAM) formation with 1*H*,1*H*,2*H*,2*H*-perfluorooctyltriethoxysilane (PFTS), blocking the vacant sites of the TiO_2 surface after dye adsorption. The F-SAM helps to efficiently lower the surface tension, resulting in efficient repelling ions, e.g., I_3^-, in the electrolyte to decrease the electron recombination rate, and the role of F-SAM is characterized in detail by impedance spectroscopy using a diffusion−recombination model. In addition, the dye aggregates on the TiO_2 surface are relaxed by the F-SAM with large conformational perturbation (i.e., helix structure) seemingly because of steric hindrance developed during the SAM formation. Such multifunctional effects suppress the electron recombination as well as the intermolecular interactions of dye aggregates without the loss of adsorbed dyes, enhancing both the photocurrent density (11.9 → 13.5 mA cm^{-2}) and open-circuit voltage (0.67 → 0.72 V). Moreover, the combined surface modification with the F-SAM and the classical coadsorbent further improves the photovoltaic performance in DSCs.

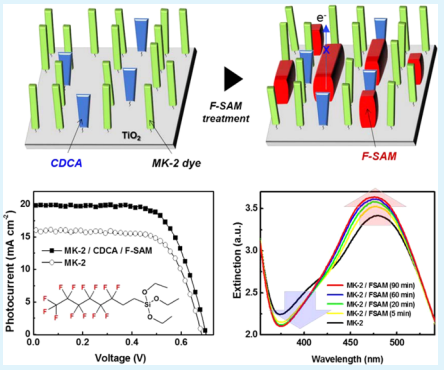

KEYWORDS: *dye-sensitized solar cell, dye aggregation, electron recombination, fluorinated self-assembled monolayer, surface engineering*

1. INTRODUCTION

Photoanodes consisting of photosensitizing dyes adsorbed on mesoporous semiconducting metal oxide layers (e.g., TiO_2) are the key element for a dye-sensitized solar cell (DSC) and have attracted the most attention for understanding the photovoltaic behavior and improving the device performance.[1−7] Adsorbed dyes are excited to generate electrons upon absorbing the solar light, injecting them into mesoporous TiO_2 layers. In this major electron generation step, the surface phenomena of the TiO_2 photoanodes play a major role, determining the energy conversion efficiency. For instance, if dyes are closely packed and subsequently aggregated on the TiO_2 surface, the injection kinetics and amount of photoelectrons are dependent upon the intermolecular interactions of dyes, mostly causing negative effects for light absorption and electron generation.[8,9] In addition, the electrons transferred to the TiO_2 layer have a tendency to back-transfer to oxidized redox couples in the electrolyte such as I_3^-, called electron recombination. Such electron recombination occurs through the vacant sites uncovered by dyes on the TiO_2 surface, deteriorating the photocurrent density and photovoltage in DSCs.[10−13]

One simple but effective way of solving the dye aggregation and electron recombination issues on TiO_2 photoanodes is to utilize coadsorbents. Chenodeoxycholic acid (CDCA),[14,15] decylphosphonic acid,[16] and dineohexylbis(3,3-dimethylbutyl)-phosphinic acid[17] are the representative coadsorbents. Those classical coadsorbents form a thin passivation layer on the vacant TiO_2 surface by competitive adsorption with dyes,

Received: August 5, 2015
Accepted: October 27, 2015

 © XXXX American Chemical Society

DOI: 10.1021/acsami.5b07211
ACS Appl. Mater. Interfaces XXXX, XXX, XXX−XXX

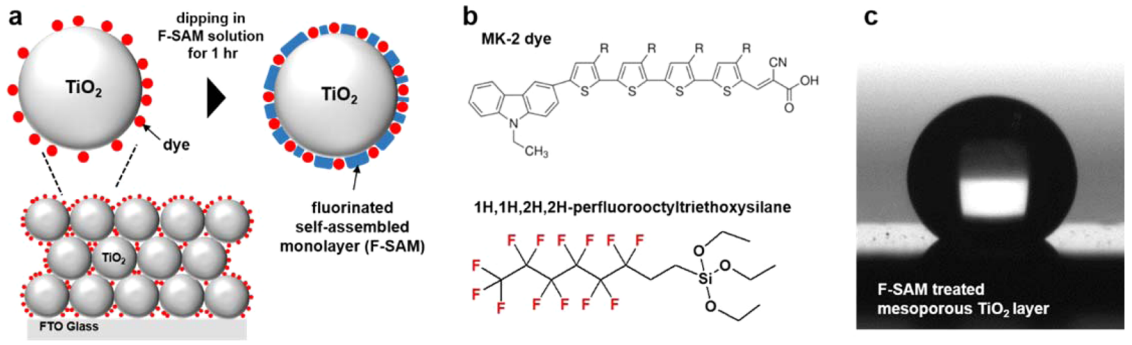

Figure 1. (a) Schematic illustration for the formation of F-SAMs on the vacant sites of a TiO_2 photoanode. (b) Chemical structures of the MK-2 dye and fluorinated carbon molecule (PFTS) for F-SAM. (c) Side-view picture of a water droplet with a 140° contact angle on the F-SAM-treated mesoporous TiO_2 film.

suppressing dye aggregation and/or electron recombination. Even though the amount of dye attached and the light-harvesting efficiency of photoanodes are obviously attenuated as a result of the competitive adsorption, the photocurrent density slightly increases in many cases.[18−21] This suggests that a decrease in the photocurrent density due to the dye loss can be compensated for by relaxing dye aggregation. However, in order to further improve the DSC performance, a relaxation strategy for the dye aggregates while keeping the amount of adsorbed dye unchanged is required. Recently, there have been some efforts to passivate the TiO_2 surface with polymers[22] or organic silanes.[23−25] Although these methods were proven to realize effective passivation on an empty TiO_2 surface, reducing the intermolecular interaction among dye aggregates while keeping the amount of dye adsorbed is still an issue to overcome.

In this context, we here introduce a surface modification strategy of TiO_2 photoanodes with a fluorinated carbon self-assembled monolayer (F-SAM) to overcome the paradoxical relationship between dye aggregation and the amount of dyes adsorbed and, at the same time, to retard electron recombination more effectively than with classical coadsorbents. A self-assembled monolayer (SAM) was formed after the dye adsorption process on the TiO_2 surface so that it could block empty TiO_2 surfaces while maintaining the amount of adsorbed dyes. Experimentally, both the F-SAM and hydrocarbon self-assembled monolayer (H-SAM) were employed, and their effects were compared to understand the photovoltaic behavior of DSCs. The surface tensions of molecules with CH_3 (30 mN m^{-1}), CF_2 (23 mN m^{-1}), and CF_3 (15 mN m^{-1}) have previously been reported.[26,27] In particular, an array of CF_3 groups at the end of the F-SAM establishes almost the minimum surface tension (below 6 mN m^{-1}) of all of the surfaces.[27] Because of the nearly minimal surface tension of modified TiO_2 surfaces, electron recombination was efficiently suppressed by blocking charged species such as I_3^- in the electrolyte to approach the empty TiO_2 surface. In addition, it was noted that the F-SAM helped to significantly perturb the dye aggregation by reducing the intermolecular interactions among the closely packed dyes adsorbed on the TiO_2 surface. Finally, we suggested a combination strategy with the F-SAM and classical coadsorbents to realize the additional energy conversion efficiency enhancement of DSCs.

2. EXPERIMENTAL SECTION

2.1. Materials. All of the chemicals were used without any further purification. Chemicals for the fabrication of DSCs and SAMs, which were 1,2-dimethyl-3-propylimidazolium iodide (DMPII), iodine (I_2), lithium iodide (LiI), 4-*tert*-butylpyridine (*t*BP), 2-cyano-3-[5‴-(9-ethyl-9*H*-carbazol-3-yl)-3′,3″,3‴,4-tetra-*n*-hexyl[2,2′,5′,2″,5″,2‴]-quaterthiophen-5-yl]acrylic acid, called MK-2 dye, triethoxy(octyl)-silane (TOS), and 1*H*,1*H*,2*H*,2*H*-perfluorooctyltriethoxysilane (PFTS) were purchased from Sigma-Aldrich. DSL 18NR-T TiO_2 pastes for mesoporous TiO_2 layers and *cis*-diithiocyanatobis(2,2′-bipyridyl-4,4′-dicarboxylato)ruthenium(II) bis(tetrabutylammonium), called N719, were obtained from Dyesol.

2.2. Fabrication and Surface Passivation of Photoanodes. Titanium(IV) bis(ethyl acetoacetato)diisopropoxide (0.1 M) in a 1-butanol solution was spin-coated onto a fluorine-doped tin oxide (FTO) glass (TEC 7, Pilkington) followed by sintering at 450 °C for the formation of an electron blocking layer (BL). TiO_2 photoanodes were first prepared by the doctor blade coating of TiO_2 pastes on the BL FTO substrates and then sintered at 450 °C for 30 min. Subsequently, the FTO substrates containing TiO_2 mesoporous films were dipped into a 40 mM $TiCl_4$ aqueous solution at 70 °C for 20 min and sintered at 450 °C for 30 min. TiO_2 photoanodes were dipped into the 0.2 mM MK-2 dye in a toluene, acetonitrile (ACN), and *tert*-butanol solution (1:1:1, v/v/v) at 30 °C for 3 h, then rinsed with toluene, and dried in vacuum conditions. For surface modification with F-SAM and H-SAM, as-prepared TiO_2 photoanodes were dipped into 0.1 M PFTS and TOS, respectively, in a hexane solution at 30 °C for 90 min and then rinsed with hexane.

2.3. Device Fabrication. Platinum (Pt) counter electrodes were fabricated by thermal decomposition of 0.01 M H_2PtCl_6 in an isopropyl alcohol solution spin-coated on FTO substrates at 450 °C for 30 min, and then two holes were drilled for electrolyte injection. The TiO_2 photoanodes were then attached with the counter electrodes using Surlyn films (25 μm thickness, Solaronix), which served as a spacer between the two electrodes. The electrolyte was a solution with 0.6 M DMPII and 0.1 M I_2 in ACN, and 0.1 M LiI and 0.5 M *t*BP were additionally mixed for the best performance cells. The mixed electrolyte was filled into the space between the photoanode and counter electrode through the holes of a Pt counter electrode by capillary force, and the holes were subsequently sealed by a Surlyn films and a thin cover glass.

2.4. Photovoltaic Performance Characterization. The optical properties of photoanodes were characterized by UV/vis spectroscopy (V-670 UV/vis spectrophotometer, Jasco). The thicknesses of the photoanodes were measured with a surface profiler (α-step IQ, Tencor). The photocurrent−voltage (J−V) characterization of DSCs was carried by a Keithley 2400 digital sourcemeter and a solar simulator equipped with a 300 W xenon arc lamp [Newport; the light intensity was calibrated with a silicon solar cell (PV Measurements, Inc.)]. In addition, the quantum efficiency of DSCs was analyzed by incident photon to current efficiency (IPCE) measurements (PV Measurements, Inc.) as a function of the wavelength. The chemical capacitance and recombination resistance of photoanodes were measured by impedance spectroscopy (IS) using an Autolab (Metrohm) under 1 sun illumination conditions. A bias potential

DOI: 10.1021/acsami.5b07211
ACS Appl. Mater. Interfaces XXXX, XXX, XXX−XXX

was applied from 0 to 1 V, and the frequency range was varied from 1 MHz to 10 mHz with a fixed amplitude of 10 mV. The obtained spectra were analyzed and fitted using *Z-View* software with equivalent circuits.

3. RESULTS AND DISCUSSION

Figure 1a shows a schematic on the formation of a F-SAM on a dyed TiO_2 photoanode. Experimentally, after adsorption of the organic MK-2 dyes on a mesoporous TiO_2 surface, a F-SAM was formed sequentially on the uncovered and vacant TiO_2 surface (i.e., MK-2/F-SAM photoanode), where the chemical structure of the MK-2 dye is shown in Figure 1b and Figure S1 (Supporting Information). F-SAM was successfully formed on the TiO_2 surface by dipping the dyed mesoporous TiO_2 layer into the PFTS solution in hexane, called the F-SAM treatment, resulting in a superhydrophobic surface.[28] A high water contact angle of 140.2° on the F-SAM-treated mesoporous TiO_2 indicates, as expected, much less surface energy of the TiO_2 layer due to CF_2 (23 mN m^{-1}) and CF_3 (15 mN m^{-1}) moieties in PFTS,[27] as shown in Figure 1c and Figure S1 (Supporting Information).

The formation of F-SAM on a TiO_2 photoanode containing preadsorbed MK-2 dyes was verified by X-ray photoelectron spectroscopy (XPS; Figure S2, Supporting Information) with a clear binding energy peak (at ~686 eV). Interestingly, the difference in the amount of dyes adsorbed on the TiO_2 surface before and after the F-SAM treatment was negligibly small (Figures S1b and S2, Supporting Information). In addition, the relative amounts of MK-2 and PFTS on the MK-2/F-SAM photoanode was quantitatively estimated (Table S1, Supporting Information) by comparing the amount of S from MK-2 dyes (with 4 sulfur atoms) and F from PFTS (with 13 fluorine atoms), respectively. The amount of PFTS attached was estimated to be around one-third of that of MK-2 (MK-2:PFTS = 1:0.32) in the MK-2/F-SAM photoanode.

Figure 2 presents the photovoltaic performances of DSCs containing SAMs on the photoanodes. H-SAMs with TOS were additionally tested for comparison with F-SAMs. The photocurrent density (J_{sc}) and open-circuit voltage (V_{oc}) of DSCs with the TiO_2 photoanode containing organic MK-2 dyes followed by the F-SAM treatment were 13.5 mA cm^{-2} and 0.72 V, respectively. These values were 13.4% (1.6 mA cm^{-2}) and 7.5% (50 mV) higher than those with only MK-2 dyes without SAMs (Table S2, Supporting Information) and also even higher than those for the photoanode treated with H-SAMs. It is thus confirmed that fluorocarbons influence more effectively the photovoltaic performances compared with hydrocarbon chains. Therefore, DSCs with the F-SAM treatment showed up as 22.5% (5.80% → 7.11%) enhancement of the energy conversion efficiency, and the external quantum efficiency was also in good agreement with the $J-V$ characteristics (Figure 2b). In addition, the F-SAM treatment was also applied to the ruthenium complex N719 dyes. The photovoltaic performances with N719 were also enhanced by the treatment with F-SAM (Figure S3, Supporting Information) at nearly the same tendency as the MK-2/F-SAM case.

In order to investigate the effects of the SAM treatment on the photoanodes of DSCs, the optical and electrochemical properties of the photoanodes were characterized. The characteristic absorption peak of MK-2 dyes in UV/vis spectra appears at around 480 nm.[31] In addition, the secondary absorption peak at around 395 nm, which is believed to be due to the H-aggregates of dyes, was also observed,[29,30] suggesting

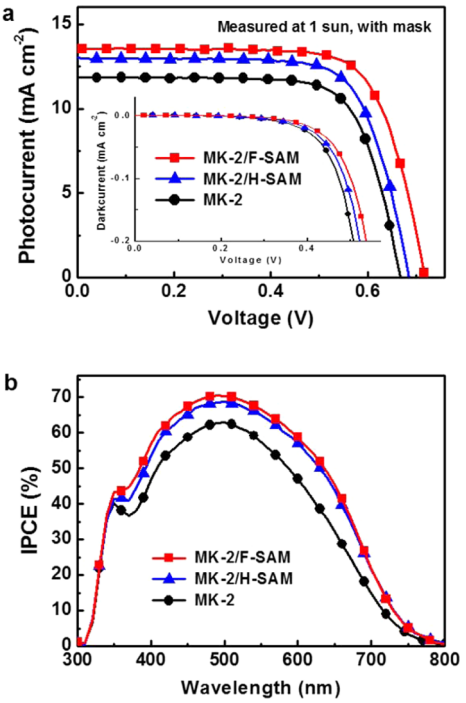

Figure 2. (a) $J-V$ characteristics and (b) IPCE spectra of DSCs based on MK-2 only sensitized (circles) and MK-2 treated with H-SAM (triangles) and F-SAM (squares) TiO_2 photoanodes under 1 sun condition (AM 1.5, 100 mW cm^{-2} solar illumination) with 0.25 cm^2 active area.

that MK-2 dyes were aggregated to some extent. H-aggregation of the dyes leads to the absorption transition by splitting the energy band gap and acts as an electron trapping site by intermolecular interactions, resulting in inefficient photoelectron generation.[8,9,30] However, after the SAM treatments, the secondary absorption peaks at around 395 nm almost disappear for both F-SAM- and H-SAM-treated photoanodes, while the main absorption peak at around 480 nm was increased at the same time, as shown in Figure 3a. It was also confirmed by variation of the UV/vis absorption peaks over the treatment time with F-SAMs, as shown in Figure 3b and Figure S4 (Supporting Information). Over the entire treatment time of the F-SAMs, the absorption at 395 nm gradually decreases, while the main absorption peak at 480 nm increases. It has previously been reported that the secondary absorption peak intensity originating from the H-aggregates of dyes was decreased by employing classical coadsorbents, but at the same time, the intensity of the main peak also decreases because of the detachment or loss of dyes.[15,18]

The UV/vis absorption behavior on the present study directly indicates that H-aggregation of the dyes was significantly mitigated by the SAM formation without the loss of dyes anchored, leading to the enhancement in J_{sc}. In addition, F-SAMs with extremely low surface energy and large conformational perturbation (i.e., helix structure) could effectively suppress H-aggregation compared with H-SAMs (zigzag structure).[31,32] Accordingly, we suggest that the SAM formation on vacant TiO_2 surface sites can cause steric hindrance and perturbations of neighboring closely arranged dyes, eventually leading to relaxation of the H-aggregates of dyes (Figure 3c).

In addition, improvement of the photovoltaic performance by employing F-SAMs in DSCs could arise from charge transfer

DOI: 10.1021/acsami.5b07211
ACS Appl. Mater. Interfaces XXXX, XXX, XXX−XXX

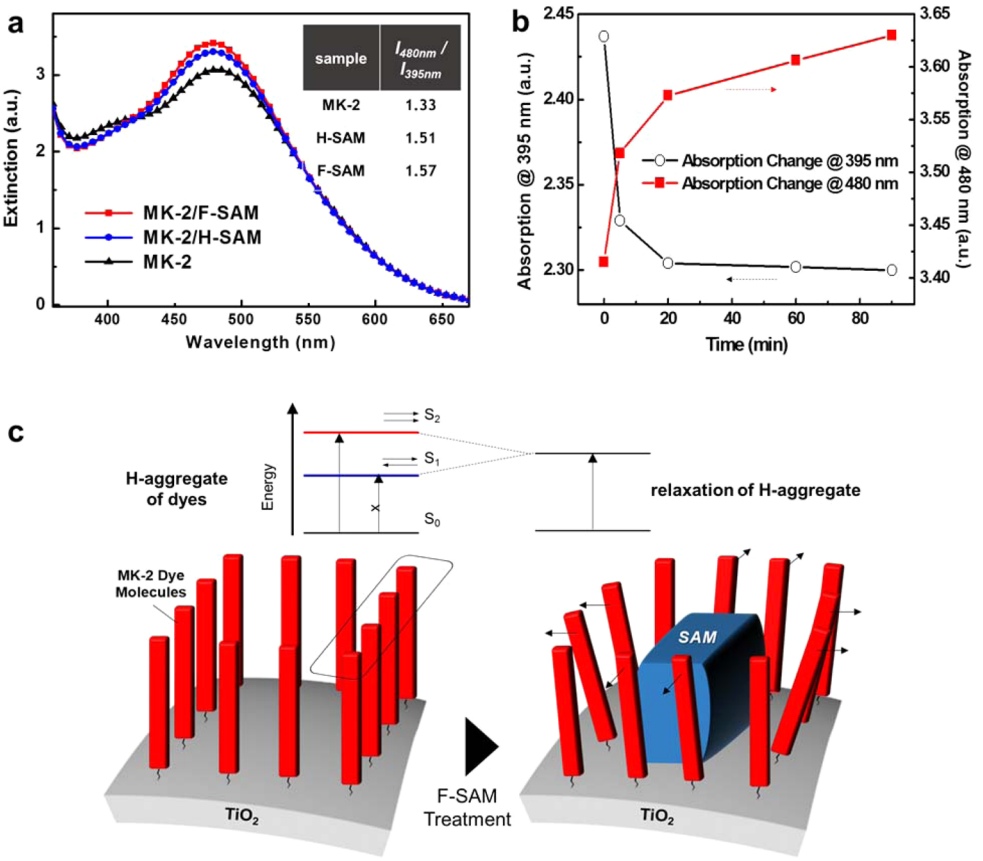

Figure 3. (a) UV/vis spectra of MK-2 dye-sensitized TiO_2 photoanodes treated with hydrocarbon (blue line) and fluorinated (red line) SAMs (inset table: relationship of the absorption peak between 395 and 480 nm). (b) Changes in the two absorption peak intensities at 395 and 480 nm as a function of the treatment time with F-SAMs. (c) Schematic illustration of the relaxation of dye aggregates by the existence of F-SAMs.

through the TiO_2/electrolyte interface, which was characterized by IS using the equivalent diffusion−recombination circuit model.[33] Figure 4a shows the change in the chemical capacitance (C_μ) as a function of the corrected voltage (V_F), yielding information on the degree of the TiO_2 conduction band (CB) shift by the SAM treatment.[34] The energy difference between the TiO_2 CB and the redox level of the electrolyte ($E_c - E_{redox}$) from the measured C_μ values was calculated as listed in Table 1.[35,36] $E_c - E_{redox}$ shows a small increment from MK-2 (0.953 eV) to MK-2/SAM photoanodes (H-SAM, 0.961 eV; F-SAM, 0.977 eV), indicating that SAM formations on the TiO_2 surface shifts the TiO_2 CB in the upward direction for the V_{oc} enhancements. It is also consistent with the previous report from De Angelis's group.[37] They suggested that the CB of TiO_2 was slightly shifted by the adsorption of coadsorbent molecules on the TiO_2 surface with below ±4 D of the dipole moment (the molecular dipole moments of H-SAM and F-SAM are 0.8 and 2.2 D, respectively[38]). Moreover, the work function results characterized by a Kelvin probe force microscope (KPFM) also confirmed the upward shift of the TiO_2 CB by SAM treatments, as shown in Figure S6 (Supporting Information). Generally, the upward shift of the TiO_2 CB reduces the electron injection efficiency and consequently decreases J_{sc}. However, the relaxation of dye aggregates upon SAM passivation compensates for the negative effect for J_{sc}, inducing even higher J_{sc} (Figure 2a and Table S2, Supporting Information).

In contrast to the results of C_μ, the recombination resistance (R_{rec}) of a MK-2/F-SAM photoanode is increased more than 1.5 times compared with the value for a MK-2-only photoanode, as shown in Figure 4b. R_{rec} was related to the recombination rate and calculated from[39,40]

$$R_{rec} = \frac{k_B T}{k_{rec} \beta L A q^2 N_c^{\beta}} \exp\left(\beta \frac{E_c - E_{redox}}{k_B T}\right) \exp\left(-\beta \frac{qV}{k_B T}\right) \quad (1)$$

where q is the elementary charge, k_B is the Boltzmann constant, T is the absolute temperature, L is the film thickness of TiO_2, A is the active cell area, and N_c of 5.0×10^{22} cm^{-3} chosen for the analysis is the effective number of states contributing to the recombination in the CB. For a more accurate analysis on the charge recombination kinetics in the photoanode, the charge recombination rate constant (k_{rec}) was calculated by using eq 1.[41] Table 1 shows that k_{rec} values are progressively decreased from MK-2-only (7.62×10^{14} $cm^{-3(1-\beta)}$ s^{-1}) to MK-2/SAM photoanodes (H-SAM, 7.34×10^{14} $cm^{-3(1-\beta)}$ s^{-1}; F-SAM, 6.90×10^{14} $cm^{-3(1-\beta)}$ s^{-1}). These data strongly reveal that electron recombination is effectively suppressed by the passivation effect of F-SAM, acting as a blocking barrier of electrons for the oxidized iodide species, I_3^-. It also indicates an increase in V_{oc} upon the incorporation of SAM formation. The suppressed electron recombination is in good agreement with the electron lifetime and Nyquist result shown in Figures 4c and S7 (Supporting Information).

Meanwhile, the free electron density (n) was estimated by Boltzmann statistics assuming that $-qV \gg k_B T$ because $n = N_c \exp(qV/k_B T)$.[42,43] n is practically the balanced outcome of the kinetic competition between charge generation and charge recombination at a photoanode.[36] As shown in Table 1, the

DOI: 10.1021/acsami.5b07211
ACS Appl. Mater. Interfaces XXXX, XXX, XXX−XXX

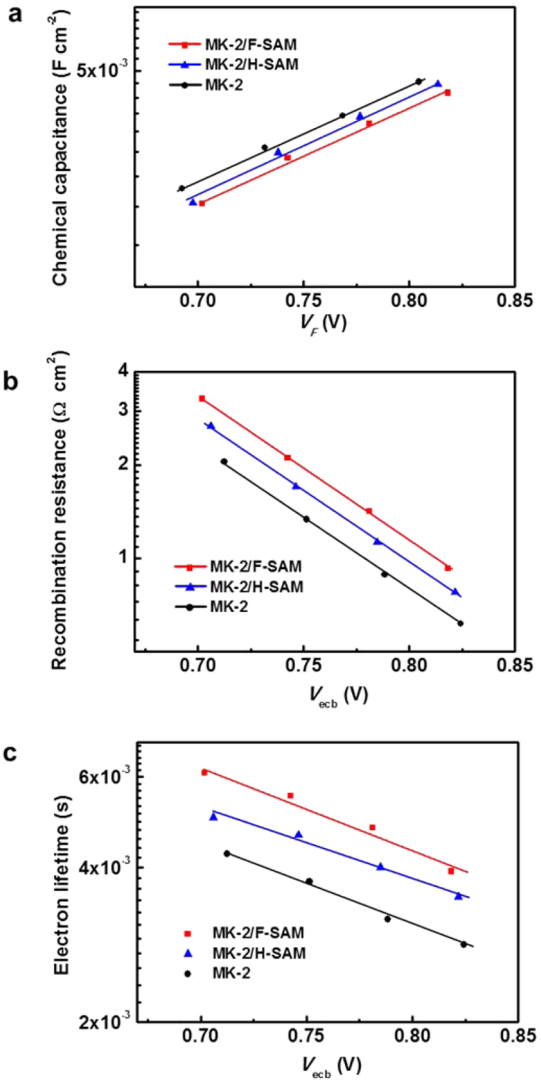

Figure 4. Electrochemical properties of TiO_2 photoanodes with MK-2 only (black circles), MK-2/H-SAM (blue triangles), and MK-2/F-SAM (red squares): (a) chemical capacitance, C_μ, with respect to the Fermi level voltage, V_F (i.e., the voltage removing the effect of series resistance); (b) recombination resistance, R_{rec}; (c) electron lifetime replotted against the equivalent common CB voltage, V_{ecb} (such that the distance between the Fermi level and the CB is the same in all cases).

calculated n of the MK-2/F-SAM photoanode (24.8×10^{17} cm^{-3}) is 3 times larger than the value for the MK-2-only photoanode (8.9×10^{17} cm^{-3}). It is noted that the increasing rate of n in MK-2/F-SAM in comparison with the MK-2-only photoanode is almost 2.5 times higher than the decreasing rate of k_{rec}, which means that electrons were more effectively generated from dye sensitizers at the MK-2/F-SAM photoanode by relaxation of dye aggregates than electron recombination from the MK-2/F-SAM photoanode to I_3^- in an electrolyte. The relationship between the charge generation and charge recombination at a photoanode is also well matched with the results of the $J-V$ data in Figure 2a.

On the basis of the beneficial properties of F-SAM treatment, we finally propose a method combining F-SAM with classical coadsorbents, CDCA, to yield further improvement in the DSC performance. After the competitive adsorption of MK-2 and CDCA on photoanodes, F-SAMs were subsequently formed on the vacant sites of a TiO_2 layer with the same dipping method as that above. Improvements in 20 mV of V_{oc} and 4 mA cm^{-2} of J_{sc} over the pristine MK-2-only photoanode were achieved by the combination of F-SAM and CDCA, leading to the 9.4% energy conversion efficiency of DSCs realized under 1 sun condition, as shown in Figure 5 and Table 2. Moreover, it was

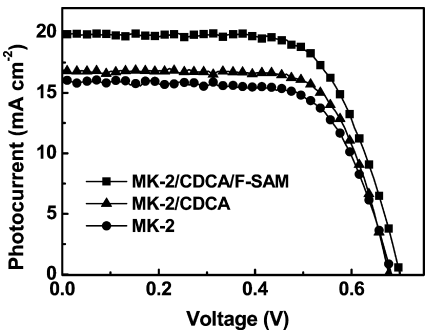

Figure 5. $J-V$ characteristics of DSCs with MK-2 (filled circles), MK-2/CDCA coadsorbed (filled triangles), and MK-2/CDCA/F-SAM (filled squares) photoanodes under 99.8 mW cm^{-2} solar illumination.

Table 2. $J-V$ Characteristics of DSCs Employing MK-2 Dyes with and without Containing CDCA and F-SAM[a]

sample	V_{oc} (V)	J_{sc} (mA cm^{-2})	FF	efficiency (%)
MK-2	0.68	15.9	0.68	7.40
MK-2/CDCA	0.68	16.9	0.71	8.09
MK-2/CDCA/F-SAM	0.70	19.9	0.67	9.41

[a]The thicknesses of the TiO_2 photoanodes were adjusted to 20 μm; measured on a 0.15 cm^2 active area.

confirmed by a long-term stability test that these improved photovoltaic performances were stably maintained for more than 14 days in Figure S8 (Supporting Information). As demonstrated in the optimal combination of CDCA and F-SAM, the F-SAM treatment suggests further enhancement of the photovoltaic performance when combined with classical coadsorbents.

Table 1. Energetic and Kinetic Parameters Calculated from the Chemical Capacitance and Recombination Resistance by IS Analysis[a]

sample	$E_c - E_{redox}$ (eV)	β	n ($\times 10^{17}$ cm^{-3})	k_{rec} ($\times 10^{14}$ cm$^{-3(1-\beta)}$ s^{-1})
MK-2	0.953	0.279	8.9	7.62
MK-2/H-SAM	0.961	0.279	14.2	7.34
MK-2/F-SAM	0.977	0.279	24.8	6.90

[a]k_{rec} is the charge recombination reaction rate constant; β is related to the charge transfer through an exponential distribution of surface states in TiO_2; E_c is the energy level of the CB in TiO_2; E_{redox} is the energy level of the electrolyte redox level.

DOI: 10.1021/acsami.5b07211
ACS Appl. Mater. Interfaces XXXX, XXX, XXX−XXX

4. CONCLUSIONS

A successful surface modification strategy with F-SAM was introduced to improve the energy conversion efficiency of DSCs. F-SAM is formed on the vacant sites of the TiO_2 photoanode surface, lowering the surface tension as well as passivating the surface to reduce the electron recombination significantly. Moreover, the role of F-SAM treatment is to perturb the H-aggregates of dyes without altering the amount of adsorbed dyes, resulting in a drastic increase in the photocurrent. Finally, upon the optimal combination of F-SAM with classical coadsorbent CDCA, the photovoltaic performance was further improved, demonstrating potential to enhance the photovoltaic performances of different types of DSCs.

■ ASSOCIATED CONTENT

Supporting Information

The Supporting Information is available free of charge on the ACS Publications website at DOI: 10.1021/acsami.5b07211.

Chemical structures of the SAM formation materials and the contact angle of water droplets on TiO_2 surfaces, XPS, UV/vis spectra, KPFM, and IS results, $J-V$ and IS results of N719-sensitized DSCs with/without F-SAM treatment, and $J-V$ characteristics under different illumination conditions (PDF)

■ AUTHOR INFORMATION

Corresponding Authors

*E-mail: kangys@hanyang.ac.kr.
*E-mail: khchar@plaza.snu.ac.kr.

Present Address

△Department of Chemistry, Faculty of Science, King Abdulaziz University, Jeddah, Saudi Arabia

Author Contributions

¶These authors contributed equally.

Notes

The authors declare no competing financial interest.

■ ACKNOWLEDGMENTS

This work was financially supported by the National Creative Research Initiative Center for Intelligent Hybrids (Grant 2010-0018290) and the IRTG program (Grant 2011-0032203) through the National Research Foundation of Korea grant and the BK21 Plus Program funded by the Ministry of Education, Science, and Technology of Korea. Additionally, this work was supported by the Korea Center for Artificial Photosynthesis (Grant 2009-0093883).

■ REFERENCES

(1) O'Regan, B.; Grätzel, M. A Low-Cost, High-Efficiency Solar Cell Based on Dye-Sensitized Colloidal TiO_2 Films. *Nature* **1991**, *353*, 737−740.

(2) Grätzel, M. Photoelectrochemical Cells. *Nature* **2001**, *414*, 338−344.

(3) Luo, Y.; Li, D.; Meng, Q. Towards Optimization of Materials for Dye-Sensitized Solar Cells. *Adv. Mater.* **2009**, *21*, 4647−4651.

(4) Grätzel, M. Recent Advances in Sensitized Mesoscopic Solar Cells. *Acc. Chem. Res.* **2009**, *42*, 1788−1798.

(5) Ito, S.; Zakeeruddin, S.; Humphry-Baker, R.; Liska, P.; Charvet, R.; Comte, P.; Nazeeruddin, M.; Péchy, P.; Takata, M.; Miura, H.; Uchida, S.; Grätzel, M. High-Efficiency Organic-Dye-Sensitized Solar Cells Controlled by Nanocrystalline-TiO_2 Electrode Thickness. *Adv. Mater.* **2006**, *18*, 1202−1205.

(6) Wooh, S.; Yoon, H.; Jung, J.-H.; Lee, Y.-G.; Koh, J. H.; Lee, B.; Kang, Y. S.; Char, K. Efficient Light Harvesting with Micropatterned 3D Pyramidal Photoanodes in Dye-Sensitized Solar Cells. *Adv. Mater.* **2013**, *25*, 3111−3116.

(7) Zhang, S.; Yang, X.; Numata, Y.; Han, L. Highly Efficient Dye-Sensitized Solar Cells: Progress and Future Challenges. *Energy Environ. Sci.* **2013**, *6*, 1443−1464.

(8) Numata, Y.; Islam, A.; Chen, H.; Han, L. Aggregation-Free Branch-Type Organic Dye with a Twisted Molecular Architecture for Dye-Sensitized Solar Cells. *Energy Environ. Sci.* **2012**, *5*, 8548−8552.

(9) Sewvandi, G.; Chen, C.; Ishii, T.; Kusunose, T.; Tanaka, Y.; Nakanishi, S.; Feng, Q. Interplay between Dye Coverage and Photovoltaic Performances of Dye-Sensitized Solar Cells Based on Organic Dyes. *J. Phys. Chem. C* **2014**, *118*, 20184−20192.

(10) Tachibana, Y.; Moser, J.; Grätzel, M.; Klug, D.; Durrant, J. Subpicosecond Interfacial Charge Separation in Dye-Sensitized Nanocrystalline Titanium Dioxide Films. *J. Phys. Chem.* **1996**, *100*, 20056−20062.

(11) Peter, L. M.; Wijayantha, K. G. U. Electron Transport and Back Reaction in Dye Sensitized Nanocrystalline Photovoltaic Cells. *Electrochim. Acta* **2000**, *45*, 4543−4551.

(12) Bisquert, J.; Fabregat-Santiago, F.; Mora-Seró, I.; Garcia-Belmonte, G.; Giménez, S. Electron Lifetime in Dye-Sensitized Solar Cells: Theory and Interpretation of Measurements. *J. Phys. Chem. C* **2009**, *113*, 17278−17290.

(13) Fabregat-Santiago, F.; Bisquert, J.; Palomares, E.; Otero, L.; Kuang, D.; Zakeeruddin, S.; Grätzel, M. Correlation between Photovoltaic Performance and Impedance Spectroscopy of Dye-Sensitized Solar Cells Based on Ionic Liquids. *J. Phys. Chem. C* **2007**, *111*, 6550−6560.

(14) Yen, Y.-S.; Lin, T.-Y.; Hsu, C.-Y.; Chen, Y.-C.; Chou, H.-H.; Tsai, C.; Lin, J. A Remarkable Enhancement of Efficiency by Co-adsorption with CDCA on the Bithiazole-Based Dye-Sensitized Solar Cells. *Org. Electron.* **2013**, *14*, 2546−2554.

(15) Yum, J.-H.; Moon, S. J.; Humphry-Baker, R.; Walter, P.; Geiger, T.; Nüesch, F.; Grätzel, M.; Nazeeruddin, M. Effect of Coadsorbent on the Photovoltaic Performance of Squaraine Sensitized Nanocrystalline Solar Cells. *Nanotechnology* **2008**, *19*, 424005.

(16) Wang, P.; Zakeeruddin, S.; Humphry-Baker, R.; Moser, J.; Grätzel, M. Molecular-scale Interface Engineering of TiO_2 Nanocrystals: Improving the Efficiency and Stability of Dye-Sensitized Solar Cells. *Adv. Mater.* **2003**, *15*, 2101−2104.

(17) Wang, M.; Li, X.; Lin, H.; Pechy, P.; Zakeeruddin, S.; Grätzel, M. Passivation of Nanocrystalline TiO_2 Junctions by Surface Adsorbed Phosphinate Amphiphiles Enhances the Photovoltaic Performance of Dye Sensitized Solar Cells. *Dalton Trans.* **2009**, *45*, 10015−10020.

(18) Yum, J.-H.; Jang, S.; Humphry-Baker, R.; Grätzel, M.; Cid, J.-J.; Torres, T.; Nazeeruddin, M. Effect of Coadsorbent on the Photovoltaic Performance of Zinc Pthalocyanine-Sensitized Solar Cells. *Langmuir* **2008**, *24*, 5636−5640.

(19) Song, H. M.; Seo, K. D.; Kang, M. S.; Choi, I. T.; Kim, S. K.; Eom, Y. K.; Ryu, J. H.; Ju, M. J.; Kim, H. K. A Simple Triaryl Amine-Based Dual Functioned Co-Adsorbent for Highly Efficient Dye-Sensitized Solar Cells. *J. Mater. Chem.* **2012**, *22*, 3786−3794.

(20) Han, L.; Islam, A.; Chen, H.; Malapaka, C.; Chiranjeevi, B.; Zhang, S.; Yang, X.; Yanagida, M. High-efficiency Dye-Sensitized Solar Cell with a Novel Co-Adsorbent. *Energy Environ. Sci.* **2012**, *5*, 6057−6060.

(21) Marinado, T.; Hahlin, M.; Jiang, X.; Quintana, M.; Johansson, E.; Gabrielsson, E.; Plogmaker, S.; Hagberg, D.; Boschloo, G.; Zakeeruddin, S.; Grätzel, M.; Siegbahn, H.; Sun, L.; Hagfeldt, A.; Rensmo, H. Surface Molecular Quantification and Photoelectrochemical Characterization of Mixed Organic Dye and Coadsorbent Layers on TiO_2 for Dye-Sensitized Solar Cells. *J. Phys. Chem. C* **2010**, *114*, 11903−11910.

(22) Lee, Y.-G.; Park, S.; Cho, W.; Son, T.; Sudhagar, P.; Jung, J. H.; Wooh, S.; Char, K.; Kang, Y. S. Effective Passivation of Nano-

DOI: 10.1021/acsami.5b07211
ACS Appl. Mater. Interfaces XXXX, XXX, XXX−XXX

structured TiO_2 Interfaces with PEG-Based Oligomeric Coadsorbents To Improve the Performance of Dye-Sensitized Solar Cells. *J. Phys. Chem. C* **2012**, *116*, 6770−6777.
(23) Feldt, S.; Cappel, U.; Johansson, E.; Boschloo, G.; Hagfeldt, A. Characterization of Surface Passivation by Poly(methylsiloxane) for Dye-Sensitized Solar Cells Employing the Ferrocene Redox Couple. *J. Phys. Chem. C* **2010**, *114*, 10551−10558.
(24) Gregg, B.; Pichot, F.; Ferrere, S.; Fields, C. Interfacial Recombination Processes in Dye-Sensitized Solar Cells and Methods To Passivate the Interfaces. *J. Phys. Chem. B* **2001**, *105*, 1422.
(25) Son, H.-J.; Wang, X.; Prasittichai, C.; Jeong, N. C.; Aaltonen, T.; Gordon, R.; Hupp, J. Glass-Encapsulated Light Harvesters: More Efficient Dye-Sensitized Solar Cells by Deposition of Self-Aligned, Conformal, and Self-Limited Silica Layers. *J. Am. Chem. Soc.* **2012**, *134*, 9537−9540.
(26) Zisman, W. Contact Angle, Wettability, and Adhesion. *Adv. Chem. Ser.* **1964**, *43*, 1.
(27) Grampel, R. Surface of Fluorinated Polymer Systems. Ph.D. Thesis, Technische Universiteit Eindhoven, Eindhoven, The Netherlands, 2002.
(28) Genzer, J.; Sivaniah, E.; Kramer, E.; Wang, J.; Körner, H.; Xiang, M.; Char, K.; Ober, C.; DeKoven, B.; Bubeck, R.; Chaudhury, M.; Sambasivan, S.; Fischer, D. The Orientation of Semifluorinated Alkanes Attached to Polymers at the Surface of Polymer Films. *Macromolecules* **2000**, *33*, 1882−1887.
(29) Bunn, C.; Howells, E. Structures of Molecules and Crystals of Fluorocarbons. *Nature* **1954**, *174*, 549−551.
(30) Wooh, S.; Koh, J. H.; Lee, S.; Yoon, H.; Char, K. Trilevel-Structured Superhydrophobic Pillar Arrays with Tunable Optical Functions. *Adv. Funct. Mater.* **2014**, *24*, 5550−5556.
(31) Koumura, N.; Wang, Z.-S.; Mori, S.; Miyashita, M.; Suzuki, E.; Hara, K. Alkyl-Functionalized Organic Dyes for Efficient Molecular Photovoltaics. *J. Am. Chem. Soc.* **2006**, *128*, 14256−14257.
(32) Peyratout, C.; Daehne, L. Aggregation of Thiacyanine Derivatives on Polyelectrolytes. *Phys. Chem. Chem. Phys.* **2002**, *4*, 3032−3039.
(33) Fabregat-Santiago, F.; Bisquert, J.; Garcia-Belmonte, G.; Boschloo, G.; Hagfeldt, A. Influence of Electrolyte in Transport and Recombination in Dye-Sensitized Solar Cells Studied by Impedance Spectroscopy. *Sol. Energy Mater. Sol. Cells* **2005**, *87*, 117−131.
(34) Fabregat-Santiago, F.; Garcia-Belmonte, G.; Mora-Seró, I.; Bisquert, J. Characterization of Nanostructured Hybrid and Organic Solar Cells by Impedance Spectroscopy. *Phys. Chem. Chem. Phys.* **2011**, *13*, 9083−9118.
(35) Barea, E.; Gónzalez-Pedro, V.; Ripollés-Sanchis, T.; Wu, H.-P.; Li, L.-L.; Yeh, C.-Y.; Diau, E. W.-G.; Bisquert, J. Porphyrin Dyes with High Injection and Low Recombination for Highly Efficient Mesoscopic Dye-Sensitized Solar Cells. *J. Phys. Chem. C* **2011**, *115*, 10898−10902.
(36) Liu, J.; Zhou, D.; Xu, M.; Jing, X.; Wang, P. The Structure−Property Relationship of Organic Dyes in Mesoscopic Titania Solar Cells: Only One Double-Bond Difference. *Energy Environ. Sci.* **2011**, *4*, 3545−3551.
(37) Ronca, E.; Pastore, M.; Belpassi, L.; Tarantelli, F.; De Angelis, F. Influence of the Dye Molecular Structure on the TiO_2 Conduction Band in Dye-Sensitized Solar Cells: Disentangling Charge Transfer and Electrostatic Effects. *Energy Environ. Sci.* **2013**, *6*, 183−193.
(38) Kobayashi, S.; Nishikawa, T.; Takenobu, T.; Mori, S.; Shimoda, T.; Mitani, T.; Shimotani, H.; Yoshimoto, N.; Ogawa, S.; Iwasa, Y. Control of Carrier Density by Self-Assembled Monolayers in Organic Field-Effect Transistors. *Nat. Mater.* **2004**, *3*, 317−322.
(39) Raga, S. R.; Barea, E.; Fabregat-Santiago, F. Analysis of the Origin of Open Circuit Voltage in Dye Solar Cells. *J. Phys. Chem. Lett.* **2012**, *3*, 1629−1634.
(40) Liu, J.; Li, R.; Si, X.; Zhou, D.; Shi, Y.; Wang, Y.; Jing, X.; Wang, P. Oligothiophene Dye-Sensitized Solar Cells. *Energy Environ. Sci.* **2010**, *3*, 1924−1928.
(41) Bai, Y.; Zhang, J.; Wang, Y.; Zhang, M.; Wang, P. Lithium-Modulated Conduction Band Edge Shifts and Charge-Transfer Dynamics in Dye-Sensitized Solar Cells Based on a Dicyanamide Ionic Liquid. *Langmuir* **2011**, *27*, 4749−4755.
(42) Bisquert, J.; Mora-Seró, I.; Fabregat-Santiago, F. Diffusion−Recombination Impedance Model for Solar Cells with Disorder and Nonlinear Recombination. *ChemElectroChem* **2014**, *1*, 289−296.
(43) Bisquert, J.; Mora-Seró, I. Simulation of Steady-State Characteristics of Dye-Sensitized Solar Cells and the Interpretation of the Diffusion Length. *J. Phys. Chem. Lett.* **2010**, *1*, 450−456.

DOI: 10.1021/acsami.5b07211
ACS Appl. Mater. Interfaces XXXX, XXX, XXX−XXX